IEEE Access
Multidisciplinary | Rapid Review | Open Access Journal

Received January 23, 2020, accepted February 29, 2020, date of publication March 3, 2020, date of current version March 12, 2020.

Digital Object Identifier 10.1109/ACCESS.2020.2978054

Augmented Ship Tracking Under Occlusion Conditions From Maritime Surveillance Videos

XINQIANG CHEN[1], (Member, IEEE), XUEQIAN XU[1], YONGSHENG YANG[1], (Senior Member, IEEE), HUAFENG WU[2], (Senior Member, IEEE), JINJUN TANG[3], AND JIANSEN ZHAO[2]

[1]Institute of Logistics Science and Engineering, Shanghai Maritime University, Shanghai 201306, China
[2]Merchant Marine College, Shanghai Maritime University, Shanghai 201306, China
[3]School of Traffic and Transportation Engineering, Central South University, Changsha 410075, China

Corresponding author: Jinjun Tang (jinjuntang@csu.edu.cn)

This work was supported in part by the National Natural Science Foundation of China under Grant 51709167, Grant 51579143, and Grant 61663027, and in part by the Shanghai Committee of Science and Technology, China, under Grant 18040501700, Grant 1829501100, and Grant 17595810300.

ABSTRACT Ship tracking provides crucial on-site microscopic kinematic traffic information which benefits maritime traffic flow analysis, ship safety enhancement, traffic control, etc., and thus has attracted considerable research attentions in the maritime surveillance community. Conventional ship tracking methods yield satisfied results by exploring distinct visual ship features in maritime images, which may fail when the target ship is partially or fully sheltered by obstacles (e.g., ships, waves, etc.) in maritime videos. To overcome the difficulty, we propose an augmented ship tracking framework via the kernelized correlation filter (KCF) and curve fitting algorithm. First, the KCF model is introduced to track ships in the consecutive maritime images and obtain raw ship trajectory dataset. Second, the data anomaly detection and rectification procedure are implemented to rectify the contaminated ship positions. For the purpose of performance evaluation, we implement the proposed framework and another three popular ship tracking models on the four typical ship occlusion videos. The experimental results show that our proposed framework successfully tracks ships in maritime video clips with high accuracy (i.e., the average root mean square error (RMSE), root mean square percentage error (RMSPE), mean absolute deviation (MAD) and mean absolute percentage error (MAPE) are less than 10), which significantly outperforms the other popular ship trackers.

INDEX TERMS Smart ship, curve fitting, kernelized correlation filter, visual ship tracking, ship occlusion.

I. INTRODUCTION

Smart ship will revolutionize the maritime shipping industry in the next decade due to the advantages of reducing ship crew risk at sea (as less crew will be deployed on-board), enhancing maritime traffic efficiency, etc. Visual ship tracking task provides fundamental information for helping smart ship make intelligent sailing decisions, and many studies have been conducted for the purpose of tackling ship tracking challenges via maritime video data. Previous academic studies suggest that visual ship tracking workflow consists of generative and discriminant models [1]. More specifically, the generative based model works in a similar logic as that of the template matching method. The generative relevant models determine ship positions by considering the region in the image which is quite similar to the input training samples. The generative models may fail to fully exploit background information in maritime images, and thus the model performance may be severely degraded under heavy background interference situations (caused by neighboring ship occlusion, water waves, etc.).

Discriminant-logic based models are proposed to mitigate the generative model weakness, which has shown great success in the ship tracking community. The discriminant relevant models extract unique ship features by learning from both positive and negative training samples, which are then employed to identify ship positions in the testing ship image sequences [2]. Teng *et al.* employed two random

The associate editor coordinating the review of this manuscript and approving it for publication was Haluk Eren.

measurement matrices to extract complementary ship feature sets to accurately track ships in the inland waterway surveillance videos [3]. Chen *et al.* proposed a robust ship tracking framework by combining multi-view and sparse representation algorithms [4]. Zhao *et al.* developed a robust ship tracking model by adaptively fusing the Camshift algorithm and structural sparse appearance features [5]. Correlation filtering based tracking frameworks, the newly emerging branch for the discriminant models, show satisfied performance (i.e., track ship at high accuracy and speed) in the manner of determining the maximum responses between the image candidate region and the training ship samples. Bolme *et al.* proposed an adaptive correlation filter for accomplishing the visual ship tracking task by transforming the initial ship image sequences into frequency domain [6]. Matos *et al.* combined an adaptive correlation filter with local re-detection features to obtain high-fidelity ship positions [7]. Similar researches can also be found in [8]–[12].

Many researchers introduced deep learning frameworks to enhance the discriminant relevant model performance [13]–[17]. Leclerc et al., proposed a ResNet architecture to recognize ship types for the purpose of robust tracking ships in maritime images [18]. Li et al., developed a spatial-temporal regularized correlation filter to address the issue of unwanted boundary effect when implementing visual tracking tasks (e.g., ship tracking) [19]. Considering the complexity and uncertainty of maritime traffic situations, the visual ship tracking task faces several bottlenecks, which are required to be addressed before entering the smart ship era [19]–[21]. The typical visual ship tracking difficulties are summarized as follows. First, ship occlusion (i.e., ship is sheltered by neighboring ships, waves, etc.) challenge is commonly observed in maritime images, which may severely degrade conventional ship tracker performance due to a few features from target ship can be exploited. Second, previous studies mainly focus on obtaining meaningful ship features from maritime surveillance images, and thus we may fail to obtain satisfied ship tracking performance when the target ship is in small imaging size (due to the difficulty of extracting informative ship features). Third, the coupled tracking challenge of occlusion and small size (i.e., the target ship is in small size and occluded by neighboring ships) is anticipated to be addressed, considering that the challenge is common in demanding ship tracking scenarios.

The KCF framework is a newly developed object tracking model, which can successfully track target by fully exploring intrinsic features from both of the true training samples (i.e., positive dataset) and background-interfered samples (i.e., negative dataset) [22]. The KCF model is considered as one of the potential models for obtaining accurate ship tracking results for smart ship. It is noted that the KCF tracking performance strongly relies on the visual ship features, and thus may fail in the ship-occlusion tracking situations. To address the issue, we propose an augmented ship tracking model to obtain robust ship tracking performance under varied ship occlusion situations. The framework includes two steps, which are obtaining raw ship tracking positions and position outlier removal. We have tested our model performance on four maritime video clips involving typical ship occlusion challenges. The remainder of the paper is organized as follows: section II introduces the proposed ship tracking framework in detail. Section III describes the ship dataset, tracking goodness measurement, and the experimental results. Section IV briefly concludes the research and illustrates potential research directions.

II. METHODOLGY

The proposed ship tracking framework (i.e., kernelized correlation filter via curve-fitting which is abbreviated as KCFC) is shown in Fig. 1, which includes ship tracking and ship position outlier correctness. More specifically, the raw ship positions in maritime images are collected with the KCF tracker. After that, we implement an outlier denoise procedure to suppress the ship anomalies and estimate positions in the ship occlusion image sequences with the curve fitting model. The above two steps are illustrated in detail in the following sections.

A. SHIP TRACKING WITH KCF MODEL

The KCF model employs the cross-correlation criterion to determine correlation similarities between the ground truth ship sample (i.e., manually labeled ship region in maritime image) and the candidate samples, and the ship tracking result with the maximum similarity value is reckoned as the ship tracking result [22]. More specifically, the trained KCF ship tracker distinguishes the target ship by obtaining the maximum stimulus response between the ship training sample (i.e., ground truth ship position in previous frame) and the current ship frame. The training ship dataset (to be fed into the KCF model) is automatically updated with the newly tracked ship position, which serves as a ship training template in the following maritime frames. The KCF algorithm for ship tracking is briefly introduced in the following section, and more details are suggested to refer to [23].

The input ship training images and labels are manually marked out in the maritime video clips, which are denoted as (p_m, q_m) with parameter m representing the image and label index. The ship tracker f(p) is iteratively trained for the purpose of minimizing the model regularization error, and the tracker f(p) is represented as the optimal solution for the linear regression problem in (1). According to the rule in previous studies [22], the optimal solution for the (1) can be obtained by minimizing the distance between the training ship sample and ship candidates in the neighboring ship frames, which is reformulated as (2). The closed form solution is considered as one of the optimal solutions for (2), which is shown in the form of (3). The input ship training patterns are mapped into feature space $\phi(p_m)$, which is represented by the kernel h. The minimal solution for (2) is considered as a linear combination of the input ship training data, and we determine the maximum response of the KCF model by the (4). The optimal solution for the KCF tracker in both the linear and nonlinear situations is re-formulated as (5). Motivated by the studies in

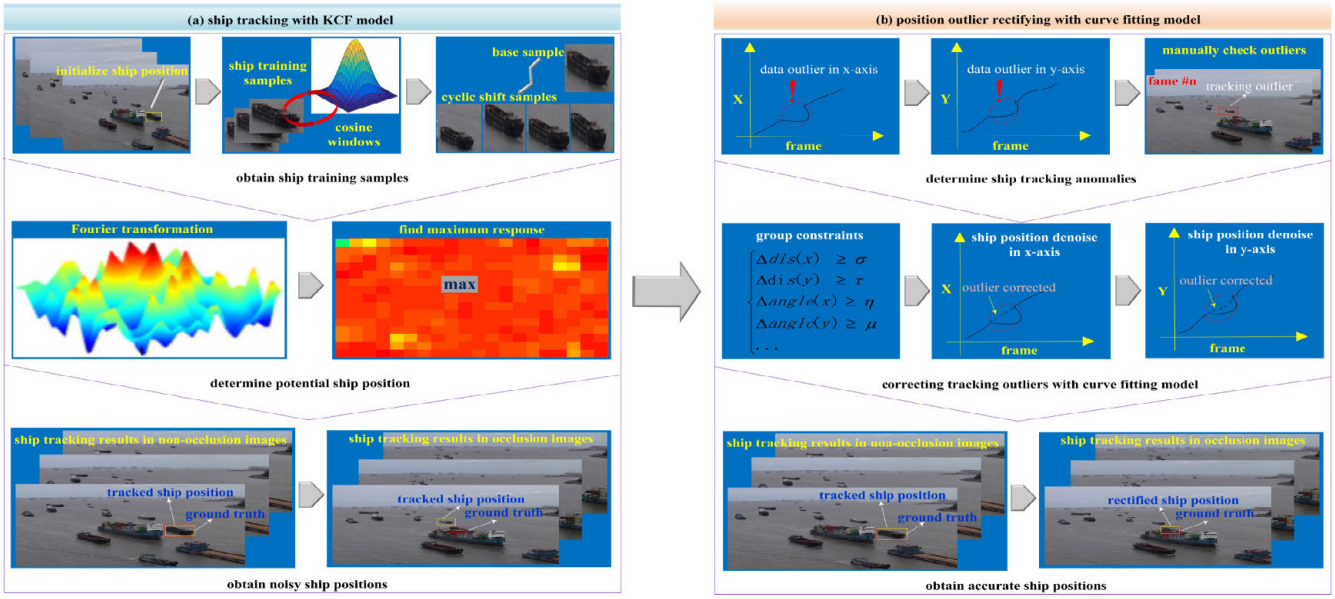

FIGURE 1. Schematic view of the proposed ship tracker.

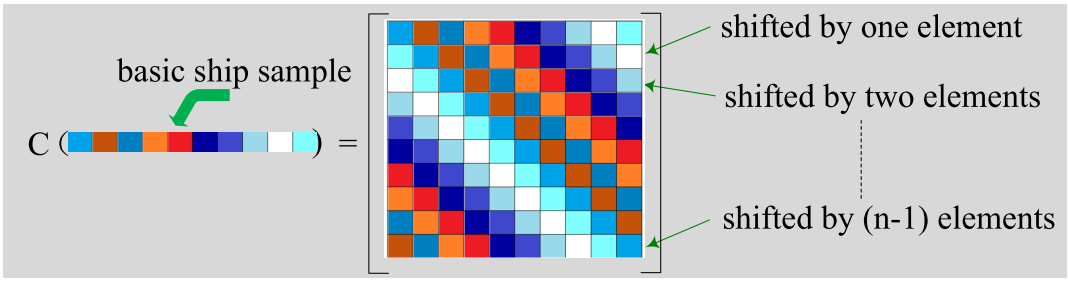

FIGURE 2. Illustration of a cyclic matrix for obtaining cyclic-shifted ship samples.

[24], [25], we can obtain a closed form solution for the KCF tracking algorithm which is shown in (6).

$$f(p) = < s, p > + c \tag{1}$$

$$\min \sum_m L(f(p_m), q_m)^2 + \lambda \|s\|^2 \tag{2}$$

$$s = (p^T p + \lambda I)^{-1} p^T q \tag{3}$$

$$s = \sum_m \alpha_m \phi(p_m) \tag{4}$$

$$f(p) = \sum_m \alpha_m h(p, p_m) \tag{5}$$

$$\alpha = (H + \lambda I)^{-1} q \tag{6}$$

where the operator $\langle \cdot, \cdot \rangle$ is a dot production, and s is considered as a linear combination of the inputs. The parameter λ determines the regularization level of the trained classifier, and the $L(f(p_m), q_m)^2$ is a loss function used for training the ship tracker. The parameter H is a kernel matrix consisting of a set of kernels h, and I is an identity matrix. The parameters p and q comprise of p_m and q_m, respectively, while the vector α represents the optimal solution for the ship tracker.

To enhance the KCF tracker generalization capability, we employ a cyclic-shift mechanism to generate additional training ship samples (see Fig. 2.). After determining the ground truth ship position in the training maritime image (which is called the base sample), the cyclic-shift mechanism is introduced to collect ship training samples by iteratively sampling on the ship base sample. More specifically, we use the cosine windows to sample on the initial ship position (i.e., the ground truth) in the training maritime frame, and thus obtain many cyclic-shift training samples. The basic permutation matrix used for obtaining cyclic-shift ship samples from maritime images (denoted as a $1 \times n$ dimensional vector $b = [b_1, b_2, b_3, \cdots, b_n]$) is shown as (7). We can obtain the circulant kernel matrix C(b) by cyclically shifting the vector b, which indeed provides us sufficient samples for training robust KCF tracker (see (8)). The C(b) can be transformed into diagonal matrix after discrete Fourier transformation (see (9)), where F is the discrete Fourier transform matrix. The input ship training samples (see (3) and (4)) can be obtained by integrated (10), where $*$ means the complex-conjugate and $\odot$ is the element-wise product.

$$m_p = \begin{bmatrix} 0 & 0 & \cdots & 0 & 1 \\ 1 & 0 & \cdots & 0 & 0 \\ 0 & 1 & \cdots & 0 & 0 \\ \vdots & \vdots & \ddots & \vdots & \vdots \\ 0 & 0 & \cdots & 1 & 0 \end{bmatrix} \tag{7}$$

$$C(b) = \begin{bmatrix} b_1 & b_2 & b_3 & \cdots & b_n \\ b_n & b_1 & b_2 & \cdots & b_{n-1} \\ b_{n-1} & b_n & b_1 & \cdots & b_{n-2} \\ \vdots & \vdots & \vdots & \ddots & \vdots \\ b_2 & b_3 & b_4 & \cdots & b_1 \end{bmatrix} \tag{8}$$

$$C(b) = F\mathrm{diag}(\hat{b})F^H \tag{9}$$

$$\hat{s} = \frac{\hat{p}^* \odot \hat{q}}{\hat{p}^* \odot \hat{p} + \lambda} \tag{10}$$

Previous studies suggest that finding the optimal solution in the temporal-spatial domain is time consuming for determining the maximal response between training ship samples and candidates [22]. To reduce the computation complexity, Gray *et al.* proposed to transform the training data and operators (ship candidates, circulant matrices, etc.) into frequency domain with the diagonalized Discrete Fourier Transform method [26]. Thus, the operations (multiplication, transposition, inversion, etc.) used for finding the maximal response can be easily implemented in pixel-wise on each training (and testing) maritime image, which is only conducted on half of the frame due to information redundancy of diagonalized Discrete Fourier Transform.

We define a compact vector Γ (see (11)) for the purpose of efficiently finding an optimal solution for the (6), which is re-formulated into (12). In that manner, the KCF model determines the potential ship area (i.e., ship position) in each of the maritime images by obtaining the maximum response between the trained model and the to-be-tracked image. More specifically, the KCF model considers the image area with minimal value in (2) as the ship tracking result, and the final ship tracking result in current ship image is shown as (13).

$$\Gamma_m = \Gamma(p, C(b)^m) \tag{11}$$

$$\alpha = F^{-1}\left(\frac{F}{F(C) + \lambda}\right) \tag{12}$$

$$q' = \sum\nolimits_m \alpha_m \Gamma(p, C(b)^m) \tag{13}$$

where Γ_m is a compact representation of kernel matrix C(b), and the division operator is implemented in element-wise, q' is the tracked ship position in current maritime frame.

B. SHIP TRACKING OUTLIER REMOVAL WITH CURVE FITTING ALGORITHM

The main weakness of tracking ships from maritime images with KCF model is that ships may be sheltered by obstacle ships moving in neighboring waterway channel, resulting in that target ship features are severely contaminated by obstacles (i.e., the KCF extracted ship features actually belong to neighboring ships), and thus leading to obvious tracking outliers. To alleviate the disadvantage, an outlier denoise procedure is implemented by firstly identifying data outlier, and then the curve fitting mechanism is introduced to estimate ship positions in the ship-occlusion image sequences according to non-occlusion ship data.

Note that ship motions at short time interval are supposed to be consistent, and thus the ship kinematic data do not change significantly in neighbouring frames. Following the assumption, we set up the group constraints in (14) to determine outliers in the raw ship tracking data. We also manually check ship tracking outliers by mapping ship positions into the corresponding ship images.

$$\begin{cases} \Delta\mathrm{dis}(x) \geq \sigma \\ \Delta\mathrm{dis}(y) \geq \tau \\ \Delta\mathrm{angle}(x) \geq \eta \\ \Delta\mathrm{angle}(y) \geq \mu \end{cases} \tag{14}$$

where $\Delta\mathrm{dis}(x)$ is ship displacement in neighboring frames in the x-axis, and $\Delta\mathrm{dis}(y)$ is the ship displacement between neighboring frames in the y-axis. The parameters $\Delta\mathrm{angle}(x)$ and $\Delta\mathrm{angle}(y)$ present ship sailing direction variation magnitude in x and y-axis, respectively. The thresholds for identifying data outlier in each equation are represented as σ, τ, η and μ, respectively.

By detecting outliers in the raw ship positions, the curve fitting model is implemented to suppress ship tracking anomalies by reconstructing ship trajectories in the ship-occlusion images. More specifically, the tracked ship positions in the non-occlusion image sequences are selected as the training data for the purpose of fine-tuning curve fitting model. Previous studies suggest that the trained curve fitting model is expected to find the minimum loss function for the (15) [27]. After that, we can estimate ship positions in the ship-occlusion images by applying the curve fitting model on the ship data series in the x and y-axis, respectively.

$$\min \sum\nolimits_{i=1}^{k} (y_c(i) - \widehat{y_c}(i))^2 + (x_c(i) - \widehat{x_c}(i))^2 \tag{15}$$

where $(x_c(i), y_c(i))$ is the tracked ship coordinate set in x and y-axis in the ith frame, and $(\widehat{x_c}(i), \widehat{y_c}(i))$ is the predicted ship position in the same frame, and k is the ship frame number.

C. FITTING GOODNESS MEASUREMENTS

To evaluate our proposed ship tracker performance, we compare the tracked ship positions with ground truth positions (which are manually marked by our group members). According to the rules in previous studies [4], [17], we employ four statistical indicators (i.e., root mean square error (RMSE), root mean square percentage error (RMSPE), mean absolute deviation (MAD), mean absolute percentage error (MAPE)) to quantify ship tracker performance. Note that each ship is presented in the form of a rectangle, both of the tracked and the ground truth positions are denoted by their center points (i.e., intersection point (IP) of each rectangle's diagonals). We evaluate tracker performance with Euclidean distance between the center points. More specifically, for a given ship video with m-frames, we employ $S(x, y)$ to represent the ground truth IP coordinates, and $L(x, y)$ for the ship tracking results. The offset between the two positions is obtained by calculating the Euclidean distance between $L(x, y)$ and $S(x, y)$ (see (16) to (18)). Thus, the RMSE, RMSPE, MAD and MAPE statistical values are obtained through (19) to (23). Smaller values for the four statistical

TABLE 1. Detailed information for the collected ship video clips.

No.	frame rate (frame per second)	resolution	length	camera position	ship tracking challenge
video #1	30 fps	1280×720	35 s	on-shore building	small-size ship completely occluded by a large-size ship
video #2	30 fps	1280×720	37 s	on-shore building	large-size ship completely occluded by a large-size ship
video #3	30 fps	1980×1080	33 s	ship stem	small-size ship partially occluded by a small-size ship
video #4	30 fps	1280×720	21 s	ship port-side	ship occlusion with mist weather condition

indicators show better tracking performance (i.e., closer to the ground truth ship positions), and vice versa.

$$\mathrm{M}_t(\mathrm{x}) = (\mathrm{S}_t(\mathrm{x}) - \mathrm{L}_t(\mathrm{x}))^2 \tag{16}$$

$$\mathrm{M}_t(\mathrm{y}) = (\mathrm{S}_t(\mathrm{y}) - \mathrm{L}_t(\mathrm{y}))^2 \tag{17}$$

$$\mathrm{M}_t(\mathrm{S}(\mathrm{x},\mathrm{y}),\mathrm{L}(\mathrm{x},\mathrm{y})) = \sqrt{\mathrm{M}_t(\mathrm{x}) + \mathrm{M}_t(\mathrm{y})} \tag{18}$$

$$\overline{\mathrm{M}} = \frac{\sum_{t=1}^{\mathrm{m}} \mathrm{M}_t(\mathrm{S}(\mathrm{x},\mathrm{y}),\mathrm{L}(\mathrm{x},\mathrm{y}))}{\mathrm{m}} \tag{19}$$

$$\mathrm{RMSE} = \sqrt{\frac{\sum_{t=1}^{\mathrm{m}} |\mathrm{M}_t(\mathrm{S}(\mathrm{x},\mathrm{y}),\mathrm{L}(\mathrm{x},\mathrm{y})) - \overline{\mathrm{M}}|^2}{\mathrm{m}}} \tag{20}$$

$$\mathrm{RMSPE} = \sqrt{\frac{1}{\mathrm{m}} \sum_{t=1}^{\mathrm{m}} \left| \frac{\mathrm{M}_t(\mathrm{S}(\mathrm{x},\mathrm{y}),\mathrm{L}(\mathrm{x},\mathrm{y})) - \overline{\mathrm{M}}}{\mathrm{M}_t(\mathrm{S}(\mathrm{x},\mathrm{y}),\mathrm{L}(\mathrm{x},\mathrm{y}))} \right|^2} \tag{21}$$

$$\mathrm{MAD} = \frac{\sum_{t=1}^{\mathrm{m}} \left| \mathrm{M}_t(\mathrm{S}(\mathrm{x},\mathrm{y}),\mathrm{L}(\mathrm{x},\mathrm{y})) - \overline{\mathrm{M}} \right|}{\mathrm{m}} \tag{22}$$

$$\mathrm{MAPE} = \frac{1}{\mathrm{m}} \sum_{t=1}^{\mathrm{m}} \left| \frac{\mathrm{M}_t(\mathrm{S}(\mathrm{x},\mathrm{y}),\mathrm{L}(\mathrm{x},\mathrm{y})) - \overline{\mathrm{M}}}{\mathrm{M}_t(\mathrm{S}(\mathrm{x},\mathrm{y}),\mathrm{L}(\mathrm{x},\mathrm{y}))} \right| \tag{23}$$

where $\mathrm{M}_t(\mathrm{x})$ represents the distance between points $\mathrm{S}(\mathrm{x},\mathrm{y})$ and $\mathrm{L}(\mathrm{x},\mathrm{y})$ on the x-axis at frame t. The symbol m is the frame number. The $\mathrm{S}_t(\mathrm{x})$ and $\mathrm{L}_t(\mathrm{x})$ are the corresponding x-coordinates. The above rule is applicable to the parameters $\mathrm{M}_t(\mathrm{y})$, $\mathrm{S}_t(\mathrm{y})$ and $\mathrm{L}_t(\mathrm{y})$. The Euclidean distance between $\mathrm{L}(\mathrm{x},\mathrm{y})$ and $\mathrm{S}(\mathrm{x},\mathrm{y})$ is represented as $\mathrm{M}_t(\mathrm{S}(\mathrm{x},\mathrm{y}),\mathrm{L}(\mathrm{x},\mathrm{y}))$, and parameter $\overline{\mathrm{M}}$ shows the average Euclidean distance.

III. EXPERIMENTS

We have implemented our proposed KCFC tracker on the four collected ship videos. Another three popular ship tracking algorithms (i.e., KCF [22], mean-shift tracker [4] and scale adaptive with multiple features (abbreviated as SAMF) tracker [21]) were tested on the same ship videos for the purpose of model performance comparison. The ship tracking experiments were conducted on the Windows 10 OS with an Intel Core I7-4710 HQ CPU @ 3.50GHz processor and RAM is 8G. The GPU version is NVIDIA GeForce GTX 850M with 2G memory. The four ship tracking modes were implemented on Matlab 2016 version.

A. DATA

For the purpose of shooting maritime videos, we installed several surveillance cameras on-board and from the on-shore buildings (i.e., ship keel, bridge, administrative building of maritime safety administration) near Shanghai Port, Shanghai, China. After carefully checking the collected video set, we found the maritime videos are easily interfered by additional imaging challenges (e.g., camera vibration, limited camera coverage). To mitigate such interferences (which are beyond our research focus in the current study), we carefully selected the four empirical ship videos from initial collected videos, where two videos were shot by the coastal building borne cameras and the remaining two by ship-borne camera. More specifically, the four ship-occlusion video clips are selected from the dataset to evaluate the proposed ship tracking model, which are denoted as video #1, video #2, video #3 and video #4. The video #1 aims for testing our model performance when the target ship is in small-imaging size, and the ship in neighboring waterway channel (i.e., the overlapping ship) is in large size. The video #1 length is 35 s, and the image resolution is 1280 × 720. The video #2 was collected by the same conditions as those of video #1 (i.e., same frame rate, resolution, weather condition, camera positions, shooting angle, etc.). The length of video #2 is 37 s, and both the target and obstacle ships are in large-size. The third video clip was shot by a ship-borne camera (the camera is installed on ship stem) when the ship was sailing near Shanghai port waterways. The video #3 contains 990 frames which were taken at 30 frame-per-second, and the image resolution is 1980 × 1080. The fourth video was shot within mist weather condition, which was captured by ship-borne camera as well. The video #4 length is 21 second and the frame rate is 30 fps with image resolution 1280 × 720. More detailed information for the collected ship-occlusion videos are shown in table 1, and some ship frame samples are shown in Fig. 3. Readers are suggested to refer to [28] for the detailed definitions of small and large ships in maritime surveillance images.

Note that the average ship speeds (i.e., the occlusion-involved ships) in our video clips is approximately 15 knot, and the ship length in maximum is 200 m. For the purpose of

FIGURE 3. Image samples for each collected video clip (green rectangle is the target ship and the red is obstacle).

better readability, we map the speeds for the two ships into 30 knot (i.e., the target ship approximately moves at 15 m/s) and 0 knot (the obstacle ship is in static state) when the ship occlusion happens, and the supposed moving distance for the target ship is 400 m (two ship lengths). In that manner, the target ship will pass the 400 m waterway segment at 15 m/s, and thus the overall time cost is about 27 s. Based on above analysis, we think the length for each of the collected video clips can cover ship occlusion procedure (each ship clip length is over 30 s), which support ship occlusion experiments implementation in our study.

B. PARAMETER DETERMINATION

We have carefully determined the parameter setups in our proposed tracker for the purpose of obtaining optimal ship tracking results. It is found that the ship tracker employs the target ship context information (i.e., textures, contours from adjacent pixels) to determine potential ship tracking results in each frame. The previous studies suggest that the padding factor E_a (neighboring image area around the target ship), interpolation factor F_{li} and spatial bandwidth S_b (proportional to the target ship size) are very crucial for the ship tracking performance [22]. To obtain satisfied parameter setups, six groups of parameter setups were carefully tested, which were (1) E_a is 1.1, F_{li} is 6.0×10^{-4}, S_b is 6.0×10^{-4}; (2) E_a is 1.1, F_{li} is 6.0×10^{-2}, S_b is 6.0×10^{-4}; (3) E_a is 1.1, F_{li} is 6.0×10^{-1}, S_b is 6.0×10^{-4}; (4) E_a is 5.0, F_{li} is 6.0×10^{-4}, S_b is 6.0×10^{-4}; (5) E_a is 5.0, F_{li} is 6.0×10^{-4}, S_b is 6.0×10^{-1}; (6) E_a is 5.0, F_{li} is 6.0×10^{-1}, S_b is 6.0×10^{-1}. The ship tracking results with different parameters were shown in Fig. 4, where the red rectangle is the ground truth ship position and the yellow rectangle indicates the ship tracking positions by the proposed framework.

The upmost three subplots in the Fig. 4 have shown that parameter F_{li} is quite important for ship tracker performance. By comparing the Fig. 4(a) to 4(c), we found larger F_{li} leads to more deteriorated tracking performance, and the tracker obvious lost the target ship when the F_{li} was set to 6.0×10^{-1} (see the Fig. 4(c)). The main reason is that the F_{li} is very sensitive to the visual appearance of the training sample from neighboring ships, and thus larger F_{li} provides the ship tracker with more trivial image information which are considered as interference. The tracking results in Fig. 4(d) to 4(f) have shown that inappropriate settings of parameters E_a and S_b can mislead the ship tracker. Taking the tracking accuracy into consideration (see the tracking results in Fig. 4(a) to 4(f)), we set default KCF parameters as follows if no further specifications stated in our research: E_a is set to 1.1, F_{li} is settled to 6.0×10^{-4}, and S_b is fixed as 6.0×10^{-4}. After carefully checking the ship tracking data distributions, we set

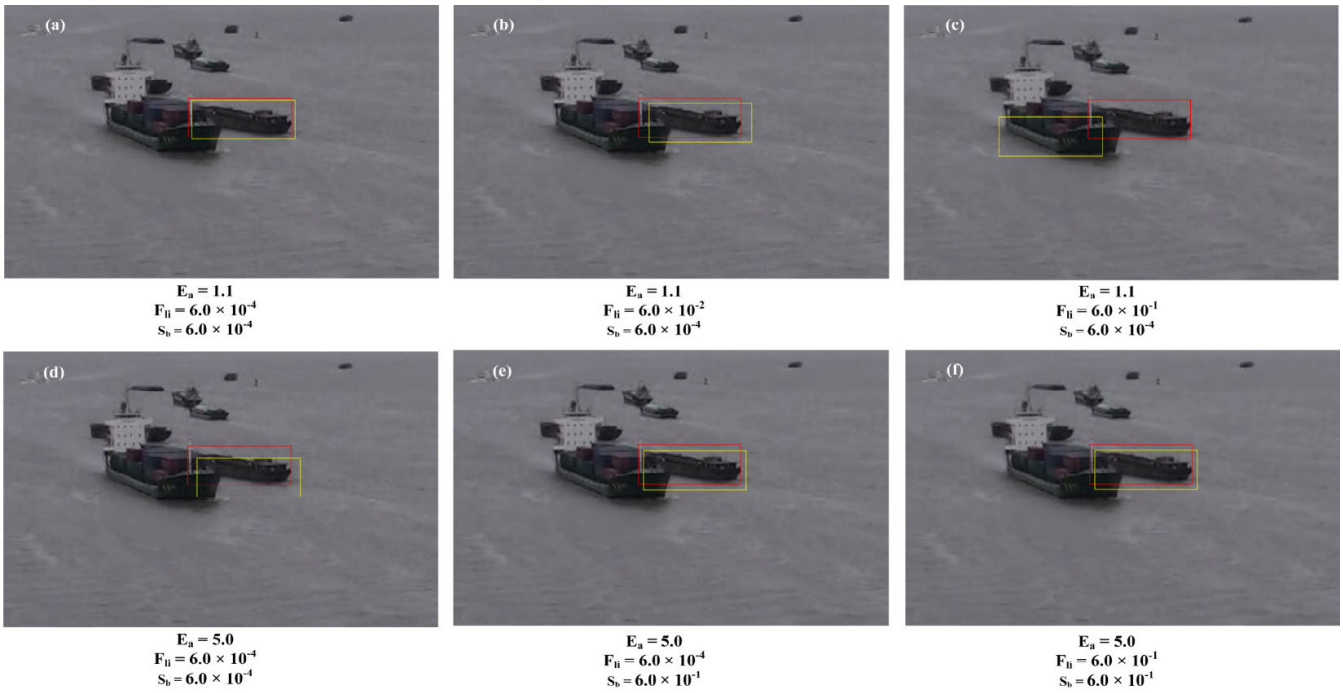

FIGURE 4. Ship tracking results with different parameter settings at frame #80 from video #1 (red rectangles are ground truth ship positions, and the yellow ones are the tracking results).

the following parameters for the purpose of identifying ship position outliers: $\sigma = 39$ pixels, $\tau = 16$ pixels, $\eta = 33^{\circ}$ and $\mu = 12^{\circ}$. Various setups were tested for the purpose of obtaining optimal parameter settings in the curve fitting model. It is found that the curve fitting model is very robust, and we set default curve fitting order into 3 without further specifications. Note that human being involvement is essential for obtaining the optimal parameter setups in our framework. The general parameters (e.g., E_a, F_{li}, S_b, etc.) are determined once in the proposed ship tracking model, and we do not need to change the values when the ship tracking challenges are not significantly different from those of our current videos.

IV. EXPERIMENTAL RESULTS

A. SHIP TRACKING RESULTS ON VIDEO #1

We have presented ship tracking results with different models in Fig. 5, where the Fig. 5(a) and 5(b) demonstrated the ship displacement in the x-axis and y-axis, respectively. Note that the ground truth, KCF, mean-shift, SAMF and KCFC ship positions are labeled as blue, green, purple, yellow and red curves in the Fig. 5. We only analyzed the ship position variation on the x-axis considering that the y-axis variation is similar to that of the x-axis. It is found that the KCF mean-shift and SAMF tracking models lost target ship (i.e., obvious outlier displacements happened in both x and y directions) when it was occluded by neighboring ships (approximately from frame #380 to #850). More specifically, the KCF tracking model was very sensitive to the ship's visual features, and thus the KCF model tracked the neighboring ship when the target ship was occluded (i.e., the features of small-size target ship can be hardly extracted by the KCF tracker).

But, the KCF tracker can re-track the ship when it was not occluded by the obstacle ship (from frame #850 to the end), and the main reason is that the KCF tracker retains the initial ship sample as tracking template for tracker training procedure. It is noted that the mean-shift tracker lost target ship, and fail to re-track the ship when the ship's visual features were not obvious observable. More specifically, the two tracking models determine ship positions by exploring ship visual features from maritime images (contours, edges, etc.), and thus ship features under occlusion scenario cannot be easily learned (i.e., small-size target ship was completely sheltered by the neighboring large-size ship). The SAMF tracked ship positions showed similar variation tendency as that of mean-shift model. After carefully checking the ship tracking results, we found that both the mean-shift and SAMF models tracked the same obstacle-ship when the target ship was occluded in the maritime image sequences.

Indeed, the KCF model learns distinct ship feature maps from both of the initial ship template and the input ship training sample, which helps the KCF tracker determine the most potential ship position in the maritime frame (i.e., the maximum response between the input ship sample and the current frame) when the ship re-enters into the camera coverage area. But, the mean-shift model obtains the ship's positions by iteratively learning from the previous ship tracking results, and thus a single frame tracking error can severely degrade ship tracking performance in latter maritime image sequences. The SAMF model have integrated different hand-crafted visual ship features into high-level ship descriptor, which may not be distinguishable when the target ship was occluded (i.e., the obstacle-ship features may be mistakenly

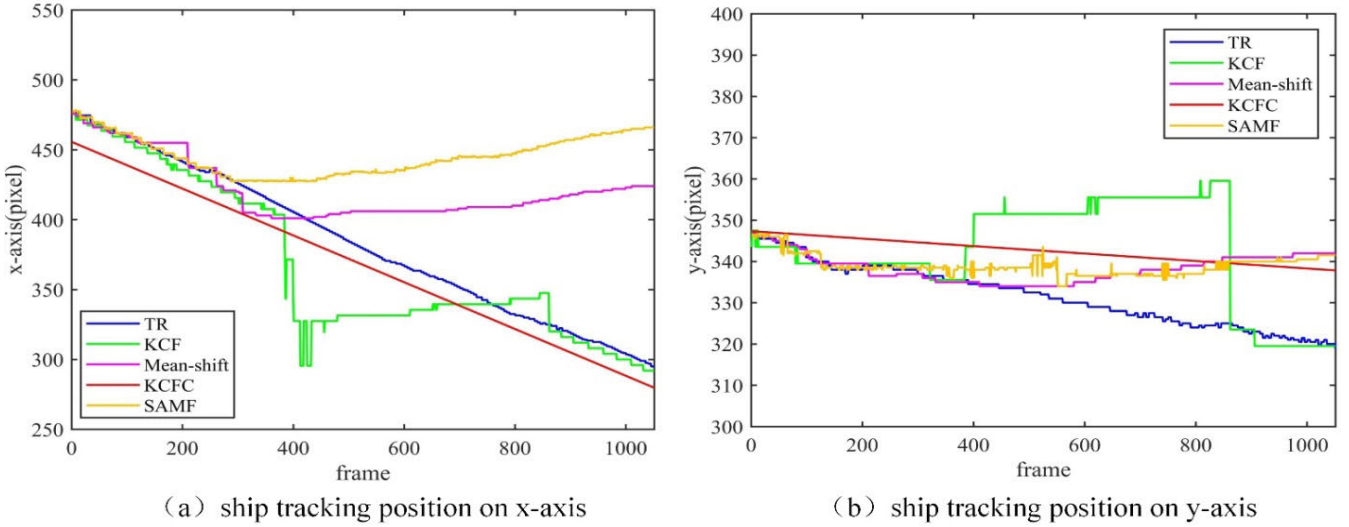

（a） ship tracking position on x-axis　　（b） ship tracking position on y-axis

FIGURE 5. Ship tracking position distributions on video #1.

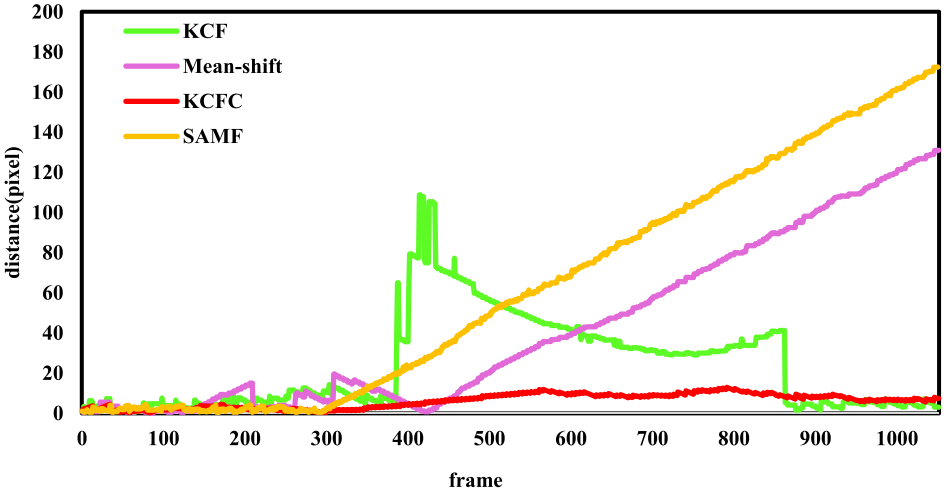

FIGURE 6. DTRGT distributions for the three tracking models for video #1.

learned by the SAMF model, and thus deteriorate SAMF tracker performance).

Our proposed ship tracking framework (i.e., the KCFC model) have successfully tackled such challenge, and obtained robust ship tracking results. More specifically, the ship positions obtained by the KCFC model are very smooth during the ship tracking procedure (see the red curve distributions in Fig. 5(a) and 5(b)). Different from the KCF and mean-shift tracking models, our proposed ship tracking model employed both ship visual feature exploration and curve fitting logics for obtaining ship positions in non-occlusion and occlusion image sequences, which integrates ship visual features and temporal-spatial information for suppressing ship occlusion anomalies. In that way, the KCFC obtained ship positions are very smooth indicating few tracking outliers. More specifically, the ship position outliers obtained in the ship-occlusion frames have been successfully removed by our proposed ship tracking model.

To quantitatively demonstrate the performance of different ship tracking models, we calculated the distance between the tracking results and the ground truth positions in each frame (which is abbreviated as DTRGT). Note that the tracker performance can be reckoned as satisfied when the average tracking error is less than 20 pixels following the rule in [4]. It is observed that the DTRGT for the mean-shift model sharply increased since 400 frames, indicating that the model failed to track the target ship (see purple curve in Fig. 6). The DTRGT curve distribution for the SAMF model showed similar tendency with that of the mean-shift model, which showed an increase tendency approximately from frame # 300 (i.e., the SAMF model showed anomaly tracking performance at frame # 300). The DTRGT distribution for the KCF tracker showed different variation tendency compared to the three counterparts. More specifically, the KCF model tracking error was negligible when the target ship was not occluded in the tracking video (i.e., the KCF tracking positions from

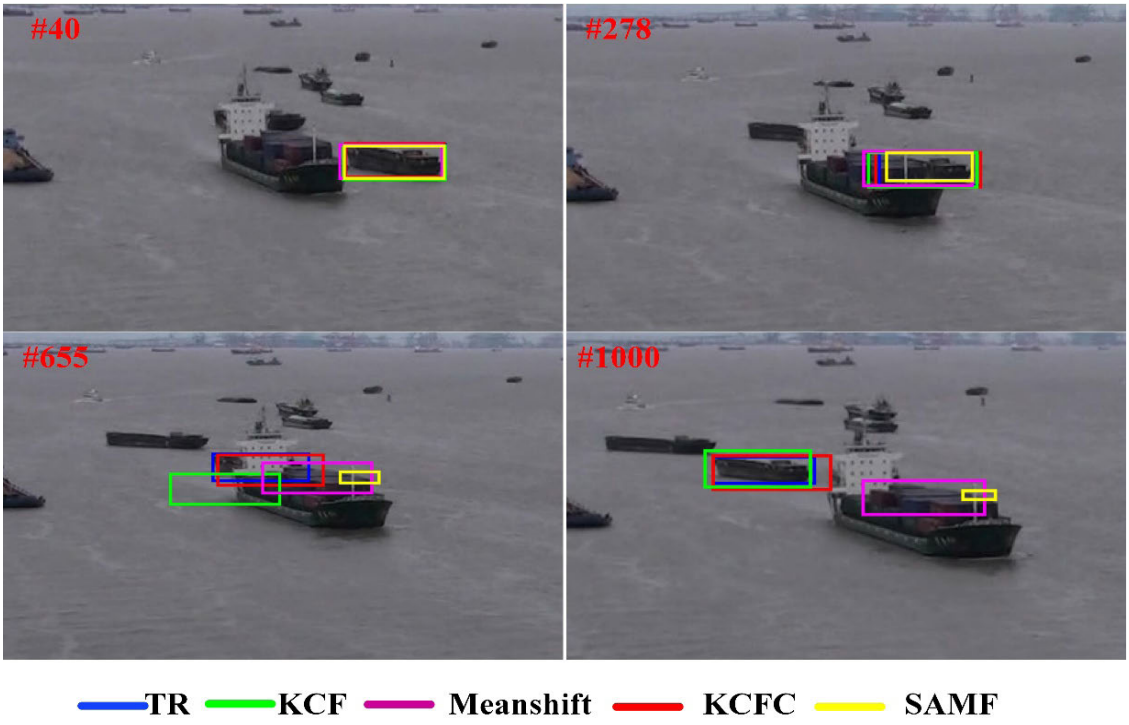

FIGURE 7. Ship tracking results for different trackers on video #1.

TABLE 2. Statistical performance for different ship tracking models on video #1.

	RMSE	RMSPE	MAD	MAPE
mean-shift	41.26	259.26	36.02	23.73
SAMF	57.01	13.45	50.56	28.42
KCF	23.12	4.82	19.79	2.83
KCFC	**3.47**	**2.39**	**3.08**	**1.21**

frame #1 to #400 and the frame #900 to #1000 are considered as very accurate due to the average DTRGT value distributions error is less than 20 pixels). The KCF tracking error in the ship occlusion frames fluctuated a lot with the maximal error reached 110 pixels. The DTRGT of our proposed ship tracker is quite small during the tracking procedure, which confirmed that our proposed ship tracker is more robust to the ship occlusion challenge in video #1.

We employed the RMSE, RMSPE, MAD, and MAPE indicators to further quantify the performance of the four ship tracking models. Compared to the other three models, the results listed in table 2 showed that the KCFC tracked ship positions are much closer to the ground truth positions on video #1. More specifically, the RMSE of the mean-shift tracking model is 41.26 pixels, which is 11.9 times larger than that of the KCFC, and the mean-shift MAD is 11.7 times larger than that of the KCFC model. The RMSPE and MAPE values for the mean-shift tracker are both significantly larger than those of our model. The SAMF obtained the largest RMSE, MAD and MAPE (which are 57.01, 13.45 and 28.42), and the RMSPE of the SAMF is the second-largest. Meanwhile, both of the RMSE and MAD values of the KCF model are ten-folds higher than that of the proposed KCFC model, considering that the MAD and RMSE indicators of the KCFC model are 3.47 and 3.08 pixels, respectively. The RMSPE and MAPE of the KCF model are 4.82 and 2.83, respectively, which are approximately two-folds higher than those of the KCFC model. From the perspective of the RMSE, RMSPE, MAD and MAPE statistics, we can draw the conclusion that our proposed ship tracking model obtained better performance than the other two models on video #1.

Typical frames of ship tracking results on video #1 are shown in Fig. 7 for the purpose of visualizing different trackers' performance. The symbol TR is the ground truth position for the target ship, and the rule is applied in the following sections without further specifications. Note that we cropped region of interest from the tracking images to clearly demonstrate the four ship trackers' performance in detail, which was applicable to the following sections without further specifications. It is observed that the four ship trackers accurately obtained ship positions at the beginning of the tracking procedure (see the tracking results of frame #40 and #278 in Fig. 7). But, the mean-shift, SAMF and KCF trackers lost the target ship in the latter two frames when the ship was sheltered by a neighboring large container ship (see the tracking results in the frames #655 and #1000). More specifically, it is observed that the mean-shift model mistakenly tracked the neighboring container ship when the target ship was lost. The KCF tracker considered the dredge ship with similar visual features as that of the target ship (i.e., the dredge ship obtained the maximal response with the

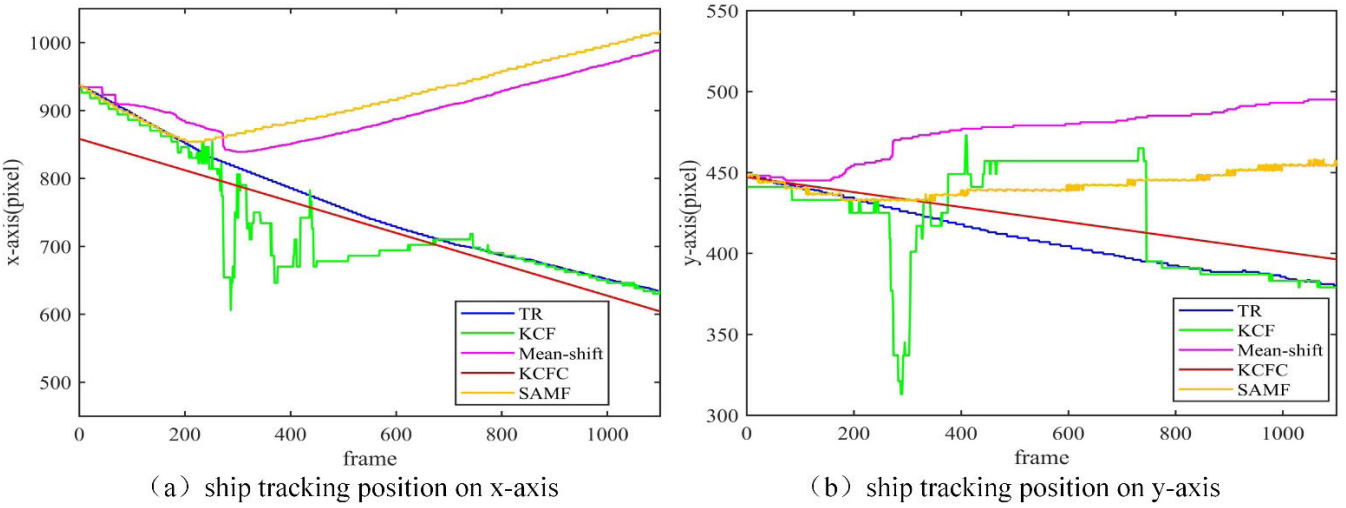

（a）ship tracking position on x-axis　　（b）ship tracking position on y-axis

FIGURE 8. Ship tracking position distributions on video #2.

tracking template in the KCF model). The SAMF tracked ship showed size-decreasing tendency in the latter frames (see the latter three subplots in Fig. 7). The main reason is that the SAMF model considered the target ship pixels which were not occluded in the image sequences as the target ship due to its scale-adaptive feature. The ship tracking results in four frames in Fig. 7 have shown that our proposed ship tracking framework successfully tracked ships (and estimated ship positions) in video #1. Based on the abovementioned experimental results and analysis, we can conclude that the proposed KCFC ship tracking model is robust to ship occlusion interference when the target ship is small and sheltered by a large neighboring ship.

1) SHIP TRACKING RESULTS ON VIDEO #2 AND #3

The proposed ship tracking model was applied on video #2 and #3 of which ship occlusion challenges are different from video #1. We do only present ship tracking results and statistical data variations for the two videos considering page limitations. The tracked ship positions (obtained by the four tracking models) and the ground truth data of video #2 and #3 were shown in Fig. 8 and 9. It is observed that the mean-shift tracking model lost the target ship approximately at frame # 270 (see the subplot of Fig. 8(a)), and the subsequently obtained ship positions showed obvious anomaly data variation. After visualizing the ship tracking results, we found that the mean-shift model wrongly tracked the neighboring container ship as the target ship (which is similar to video #1). The y-axis coordinate series of the video #2, tracked by the mean-shift tracker, varied smoothly due to that the wrongly tracked ship moved slowly in the y-direction. The KCF tracking results showed that it failed to track ship when the target ship was occluded in the image sequences frame # 300 to # 700 (see the green curves in Fig. 8(a) and 8(b)). The SAMF tracker showed obvious tracking outlier in x-axis since frame # 200, and the y-axis tracking error was observed approximately from frame #260.

The three ship trackers' performance on the video #3 showed very similar results as video #2 (see Fig. 9). More specifically, our proposed ship tracking model has extracted satisfied ship trajectories compared to ground truth position data as shown in the red curves in the Fig. 8 and 9, respectively. When zooming out the details of the ship occlusion positions, we found that, in some cases, the KCFC obtained ship position curves showed slightly inconsistent with ground truth (i.e., the ship position variation is smoother than the ground truth data as shown in subplots inside the Fig. 9(a) and 9(b), respectively). The main reason is that the curve fitting module in the proposed ship tracking model assumed that the ship tracking positions in neighboring frames are to be in small variations.

The statistical indicator distributions for the two video clips were shown in the table 3 and 4, respectively, which indicated that our proposed ship tracker can handle typical ship occlusion challenges. More specifically, the RMSE value for the KCFC model is 13.17 (6.87) pixels in video #2 (#3), which is approximately one-third to that of the KCF model counterparts for both of video #2 and #3. The RMSE for the mean-shift model is nine times higher than the KCFC counterpart in video #2, and approximately twenty times higher than that of KCFC in video #3. The MAD indicator for the two videos has shown similar variation as those of the RMSE indicator. More specifically, the minimal MAD in video #2 and #3 are 9.55 and 4.50 pixels, respectively, which were both obtained by the KCFC model. The RMSPE and MAPE indicators verified that the KCFC model obtained the minimal errors (which are 0.86 and 1.49, respectively) in comparison with the other two tracking models. Based on the RMSE, RMSPE, MAD and MAPE distribution analysis on video #2 and #3, we can conclude that the KCF, mean-shift and SAMF models may not successfully handle the ship occlusion difficulties, while the proposed KCFC ship tracking model demonstrates its efficacy on the tracking challenges.

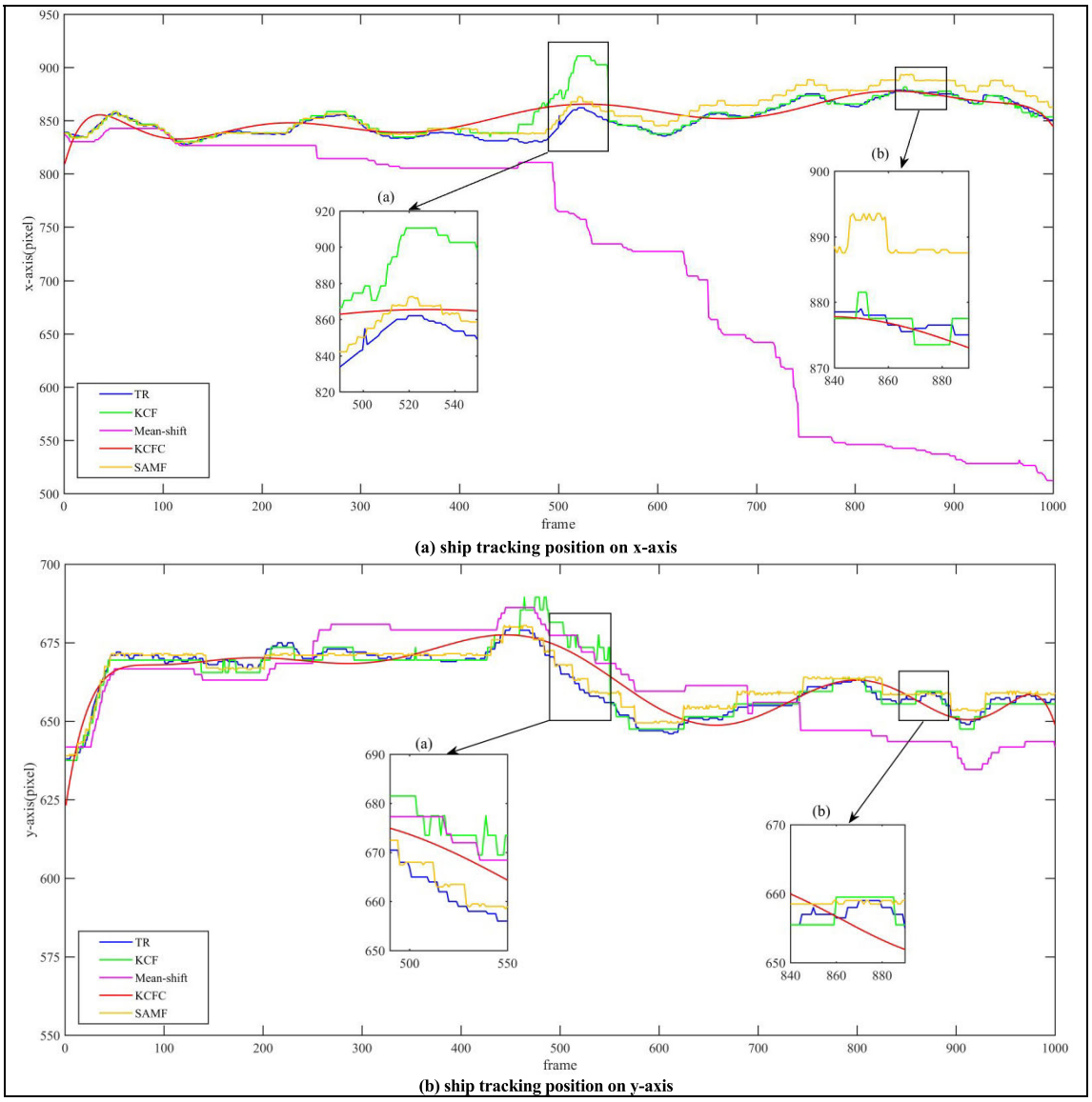

FIGURE 9. Ship tracking position distributions on video #3.

TABLE 3. Statistical performance for different ship tracking models on video #2.

	RMSE	RMSPE	MAD	MAPE
mean-shift	116.23	5.08	103.20	22.45
SAMF	52.51	17.78	113.36	49.96
KCF	41.31	6.04	33.47	12.45
KCFC	**13.17**	**0.86**	**9.55**	**1.49**

TABLE 4. Statistical performance for different ship tracking models on video #3.

	RMSE	RMSPE	MAD	MAPE
mean-shift	131.19	5.26	117.34	10.57
SAMF	15.13	1.86	5.19	3.74
KCF	17.33	2.75	7.60	3.97
KCFC	**6.87**	**1.77**	**4.50**	**2.61**

2) SHIP TRACKING RESULTS ON VIDEO #4

We collected a ship-occlusion video clip under mist weather condition (i.e. video #4) for the purpose of further verifying ship tracker robustness. The tracked ship position distributions and statistic indicators were shown in table 5 and Fig. 10, respectively. Overall, the mean-shift model showed obvious tracking performance loss in comparison with the remaining three trackers (i.e., the SAMF, KCF and KCFC models) considering that the RMSE, RMSPE, MAD and MAPE statistics for the mean-shift tracker were significantly larger than those of the counterparts. Moreover, table 5 indicated that the proposed KCFC tracker obtained

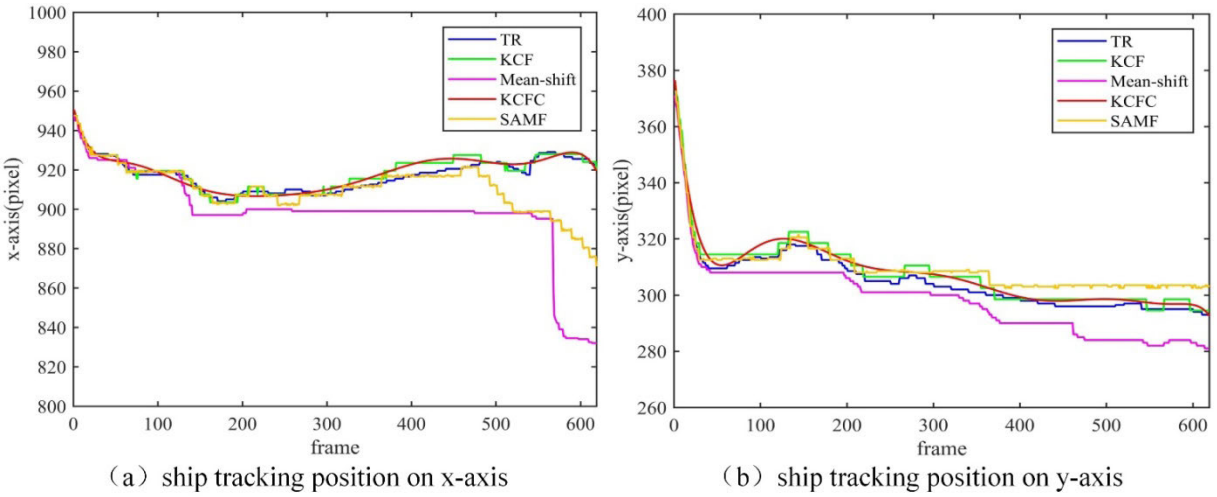

FIGURE 10. Ship tracking position distributions on video #4.

TABLE 5. Statistical performance for different ship tracking models on video #4.

	RMSE	RMSPE	MAD	MAPE
mean-shift	22.74	2.92	14.43	1.47
SAMF	11.85	3.73	8.57	2.17
KCF	1.75	0.98	1.46	0.58
KCFC	**1.49**	**0.71**	**1.26**	**0.44**

minimal tracking error as the RMSE, RMSPE, MAD and MAPE were 1.49, 0.71, 1.26 and 0.44. The ship tracking positions obtained by the KCFC model (see the red curves in Fig. 10(a) and (b)) were closer to the ground truth. In light of above analysis, we consider that our proposed ship tracker is robust to the typical ship occlusion challenges. We did not compare our model on the public computer vision datasets (e.g., VOT) due to that ship occlusion challenge is not easily observed in such dataset. To rich the diversity of the computer vision benchmarks, we are willing to share our collected video clips with interested readers by request.

V. CONCLUSION

Visual ship tracking task provides crucial on-spot kinematic traffic data which greatly benefits maritime safety and traffic efficiency in smart ship era. Ship occlusion challenge is considered as one of the bottlenecks for obtaining high-resolution maritime traffic awareness data for smart ship due to the complex and unpredictable maritime navigation environment. To that aim, we proposed a novel framework for robustly tracking ships under varied ship occlusion scenarios. More specifically, the framework employed the conventional KCF method to obtain raw ship positions, and then the ship data was rectified with curve fitting model. The experiments were conducted on four typical ship occlusion scenarios. The statistical indicators have shown that our proposed framework obtained more satisfied ship tracking performance on the collected video slips (i.e., the average RMSE, RMSPE, MAD and MAPE are 6.25 1.43, 4.60 and 1.44).

Though the proposed method achieved satisfied ship tracking accuracy under typical ship occlusion challenges, the following research work can be done to potentially enhance our framework performance. First, the weather conditions in the three collected ship videos were in good state (e.g., good visibility, windless, etc.). Testing and improving our model on the videos shot under different maritime conditions (e.g., extreme weather, lighting variation, heavy clutter interference, etc.) can provide more holistic performance evaluation results. Second, our model worked well under single ship tracking occlusion challenge, and evaluate the model performance with multiple ship occlusion tracking challenge is in need. Third, tracking ship with varied imaging scale in image sequences can be an interesting exploration in future. Fourth, we can enrich our maritime video clips (e.g., enlarging the evaluation video datasets) to further demonstrate our proposed framework performance. Last but not least, we have estimated the average ship tracking speeds on the three trackers, and found that the tracking speed for the KCF model is higher than those of the other three trackers. More specifically, the average KCF tracking speed (in terms of time cost) is approximately two-folds higher than those of the Meanshift, SAMF and KCFC models. Thus, reducing the computation complexity is considered as one of potential work in future.

REFERENCES

[1] M. Kristan, J. Matas, A. Leonardis, M. Felsberg, L. Cehovin, G. Fernandez, T. Vojir, G. Hager, G. Nebehay, R. Pflugfelder, A. Gupta, A. Bibi, A. Lukezic, A. Garcia-Martin, A. Saffari, A. Petrosino, and A. S. Montero, "The visual object tracking VOT2015 challenge results," in *Proc. IEEE Int. Conf. Comput. Vis. Workshop (ICCVW)*, Dec. 2015, pp. 564–586.

[2] S. Liu, T. Zhang, X. Cao, and C. Xu, "Structural correlation filter for robust visual tracking," in *Proc. IEEE Conf. Comput. Vis. Pattern Recognit. (CVPR)*, Jun. 2016, pp. 4312–4320.

[3] F. Teng and Q. Liu, "Robust multi-scale ship tracking via multiple compressed features fusion," *Signal Process., Image Commun.*, vol. 31, pp. 76–85, Feb. 2015.
[4] X. Chen, S. Wang, C. Shi, H. Wu, J. Zhao, and J. Fu, "Robust ship tracking via multi-view learning and sparse representation," *J. Navigat.*, vol. 72, no. 1, pp. 176–192, 2019.
[5] H. Zhao, K. Xiang, S. Cao, and X. Wang, "Robust visual tracking via CAMShift and structural local sparse appearance model," *J. Vis. Commun. Image Represent.*, vol. 34, pp. 176–186, Jan. 2016.
[6] D. Bolme, J. R. Beveridge, B. A. Draper, and Y. M. Lui, "Visual object tracking using adaptive correlation filters," in *Proc. IEEE Comput. Soc. Conf. Comput. Vis. Pattern Recognit.*, Jun. 2010, pp. 2544–2550.
[7] J. Matos, A. Bernardino, and R. Ribeiro, "Robust tracking of vessels in oceanographic airborne images," in *Proc. OCEANS MTS/IEEE Monterey*, Sep. 2016, pp. 1–10.
[8] K. Hu, J. Ye, E. Fan, S. Shen, L. Huang, and J. Pi, "A novel object tracking algorithm by fusing color and depth information based on single valued neutrosophic cross-entropy," *J. Intell. Fuzzy Syst.*, vol. 32, no. 3, pp. 1775–1786, Feb. 2017.
[9] C. Zhao, J. Yuan, and H. Zheng, "A robust object tracking method based on CamShift for UAV videos," in *Proc. Int. Conf. Intell. Data Eng. Automated Learn.*, Oct. 2017, pp. 53–62.
[10] Z. Pan, S. Liu, and W. Fu, "A review of visual moving target tracking," *Multimedia Tools Appl.*, vol. 76, no. 16, pp. 16989–17018, 2017.
[11] B. Bai, B. Zhong, G. Ouyang, P. Wang, X. Liu, Z. Chen, and C. Wang, "Kernel correlation filters for visual tracking with adaptive fusion of heterogeneous cues," *Neurocomputing*, vol. 286, pp. 109–120, Apr. 2018.
[12] J. Tang, F. Gao, F. Liu, and X. Chen, "A denoising scheme-based traffic flow prediction model: Combination of ensemble empirical mode decomposition and fuzzy C-Means neural network," *IEEE Access*, vol. 8, pp. 11546–11559, 2020.
[13] W.-C. Hu, C.-Y. Yang, and D.-Y. Huang, "Robust real-time ship detection and tracking for visual surveillance of cage aquaculture," *J. Vis. Commun. Image Represent.*, vol. 22, no. 6, pp. 543–556, Aug. 2011.
[14] P. Zhang, K. Wang, Z. Ling, Z. Xie, and L. Zhou, "An evolutionary vulnerability detection method for HFSWR ship tracking algorithm," in *Proc. Asia–Pacific Conf. Simulated Evol. Learn.*, 2017, pp. 763–773.
[15] G. Wu, W. Lu, G. Gao, C. Zhao, and J. Liu, "Regional deep learning model for visual tracking," *Neurocomputing*, vol. 175, pp. 310–323, Jan. 2016.
[16] X. Chen, L. Qi, Y. Yang, Q. Luo, O. Postolache, J. Tang, and H. Wu, "Video-based detection infrastructure enhancement for automated ship recognition and behavior analysis," *J. Adv. Transp.*, vol. 2020, pp. 1–12, Jan. 2020.
[17] X. Chen, Y. Yang, S. Wang, H. Wu, J. Tang, J. Zhao, and Z. Wang, "Ship type recognition via a Coarse-to-Fine cascaded convolution neural network," *J. Navigat.*, pp. 1–20, Feb. 2020.
[18] M. Leclerc, R. Tharmarasa, M. C. Florea, A.-C. Boury-Brisset, T. Kirubarajan, and N. Duclos-Hindie, "Ship classification using deep learning techniques for maritime target tracking," in *Proc. 21st Int. Conf. Inf. Fusion (FUSION)*, Jul. 2018, pp. 737–744.
[19] F. Li, C. Tian, W. Zuo, L. Zhang, and M.-H. Yang, "Learning spatial-temporal regularized correlation filters for visual tracking," in *Proc. IEEE Conf. Comput. Vis. Pattern Recognit.*, 2018, pp. 4904–4913.
[20] D. Chen, Z. Yuan, Y. Wu, G. Zhang, and N. Zheng, "Constructing adaptive complex cells for robust visual tracking," in *Proc. IEEE Int. Conf. Comput. Vis.*, Dec. 2013, pp. 1113–1120.
[21] Y. Li and J. Zhu, "A scale adaptive kernel correlation filter tracker with feature integration," in *Proc. Eur. Conf. Comput. Vis.*, vol. 8926, 2015, pp. 254–265.
[22] J. F. Henriques, R. Caseiro, P. Martins, and J. Batista, "High-speed tracking with kernelized correlation filters," *IEEE Trans. Pattern Anal. Mach. Intell.*, vol. 37, no. 3, pp. 583–596, Mar. 2015.
[23] K. Yang, X. Wu, Z. Zhu, J. Xu, Z. Wan, Y. Chang, and Z. Du, "A high-confidence model updating correlation filtering tracker with scale adaptation for visual target tracking," *Optik*, vol. 202, Feb. 2020, Art. no. 163730.
[24] A. J. Smola and B. Schölkopf, "A tutorial on support vector regression," *Statist. Comput.*, vol. 14, no. 3, pp. 199–222, Aug. 2004.
[25] C. S. Ong, A. J. Smola, R. C. Williamson, and R. Herbrich, "Learning the kernel with hyperkernels," *J. Mach. Learn. Res.*, vol. 6, pp. 1043–1071, Jul. 2005.
[26] R. M. Gray, "Toeplitz and circulant matrices: A review," *Found. Trends Commun. Inf. Theory*, vol. 2, no. 3, pp. 155–239, 2005.
[27] X. Wan, Y. Li, C. Xia, M. Wu, J. Liang, and N. Wang, "A T-wave alternans assessment method based on least squares curve fitting technique," *Measurement*, vol. 86, pp. 93–100, May 2016.
[28] H. Deng, X. Sun, M. Liu, C. Ye, and X. Zhou, "Infrared small-target detection using multiscale gray difference weighted image entropy," *IEEE Trans. Aerosp. Electron. Syst.*, vol. 52, no. 1, pp. 60–72, Feb. 2016.

XINQIANG CHEN (Member, IEEE) received the Ph.D. degree in traffic information engineering and controlling from Shanghai Maritime University, China, in 2018. From September 2015 to September 2016, he was a Visiting Student with the Smart Transportation Applications and Research Laboratory (STAR Lab), University of Washington, Seattle, WA, USA. He is currently a Lecturer with the Institute of Logistics Science and Engineering, Shanghai Maritime University. His research interests include traffic data analysis, transportation image processing, intelligent transportation systems, computer-vision-based transportation detection and its applications, smart ships, smart ports, and machine learning. He serves as an Editorial Board Member of five international journals and on the technical program committee for six international conferences.

XUEQIAN XU received the bachelor's degree in measurement and control technology and instruments from the School of Automation Engineering, Shanghai University of Electric Power, Shanghai, China. He is currently pursuing the master's degree in control theory and control engineering from the Institute of Logistics Science and Engineering, Shanghai Maritime University, Shanghai. He has published one article in EI-indexed international conference and applied for two patents. His research interests include maritime image processing, ship tracking, and ship behavior analysis.

YONGSHENG YANG (Senior Member, IEEE) received the Ph.D. degree from the Nanjing University of Aeronautics and Astronautics, China, in 1998. He is currently a Professor with Shanghai Maritime University. He also serves as the General Chair for the International Symposium on Sensors and Instrumentation in IoT Era 2018 and 2019 (ISSI 2018 and ISSI 2019). He is the author or coauthor of more than 50 technical articles and proceedings. His research interests include operation and optimization of port logistics, cooperated job scheduling, and automatic terminals controlling. He serves as an Associate Editor for the *International Journal of Computer Aided Engineering and Technology*.

HUAFENG WU (Senior Member, IEEE) received the Ph.D. degree in computer science from Fudan University, in 2009, and the master's degree in traffic information engineering and controlling from Dalian Maritime University, in 2004. He conducted Postdoctoral Research at Carnegie Mellon University, from 2008 to 2009. He was a Visiting Scholar with Shanghai Jiao Tong University, from 2012 to 2013. He has authored or coauthored more than 60 journal and conference papers. He is currently a Professor and a Ph.D. Supervisor with the Merchant Marine College, Shanghai Maritime University. His research interests include the Internet of Shipping, the Internet of Things, wireless sensor networks, and marine search and rescue. He also serves as an Editorial Board Member for the *Computer Communications* journal. He serves as a reviewer for many international journals in the computer science relevant field.

JINJUN TANG received the B.S. and M.S. degrees from the Shandong University of Technology, Zibo, China, in 2006 and 2009, respectively, and the Ph.D. degree in traffic information engineering and control from the Harbin Institute of Technology, Harbin, China, in 2016. He was a Visiting Student with the University of Washington, Seattle, WA, USA, from 2014 to 2016. He is currently an Associate Professor with Central South University. He has published over 30 technical articles in journals and conference proceeding as the first author or coauthor. His research interests include traffic flow prediction, data mining in transportation systems, intelligent transportation systems, and transportation modeling.

JIANSEN ZHAO received the Ph.D. degree in marine engineering from Dalian Maritime University, Dalian, China, in 2013. He is currently an Associate Professor with the Merchant Marine College, Shanghai Maritime University, Shanghai, China. He has published more than 20 articles in international journals and conferences. His current research interests include intelligent navigation, plasma antennas, gas discharge, AIS antennas, and GNSS antennas.